

# Sparse Attention as Compact Kernel Regression

Saul Santos<sup>1,2</sup> Nuno Gonçalves<sup>1,2,3</sup> Daniel C. McNamee<sup>4</sup> Marcos Treviso<sup>1,2</sup> André F.T. Martins<sup>1,2,5</sup>

## Abstract

Recent work has revealed a link between self-attention mechanisms in transformers and test-time kernel regression via the Nadaraya-Watson estimator, with standard softmax attention corresponding to a Gaussian kernel. However, a kernel-theoretic understanding of *sparse* attention mechanisms is currently missing. In this paper, we establish a formal correspondence between sparse attention and *compact* (bounded support) kernels. We show that normalized ReLU and sparsemax attention arise from Epanechnikov kernel regression under fixed and adaptive normalizations, respectively. More generally, we demonstrate that widely used kernels in nonparametric density estimation—including Epanechnikov, biweight, and triweight—correspond to  $\alpha$ -entmax attention with  $\alpha = 1 + \frac{1}{n}$  for  $n \in \mathbb{N}$ , while the softmax/Gaussian relationship emerges in the limit  $n \rightarrow \infty$ . This unified perspective explains how sparsity naturally emerges from kernel design and provides principled alternatives to heuristic top- $k$  attention and other associative memory mechanisms. Experiments with a kernel-regression-based variant of transformers—Memory Mosaics—show that kernel-based sparse attention achieves competitive performance on language modeling, in-context learning, and length generalization tasks, offering a principled framework for designing attention mechanisms.

## 1. Introduction

Self-attention is a central component of transformer architectures, enabling models to capture long-range dependencies within sequences (Vaswani et al., 2017). A growing body of work has established connections between

<sup>\*</sup>Equal contribution <sup>1</sup>Instituto Superior Técnico, Universidade de Lisboa, Lisbon, Portugal <sup>2</sup>Instituto de Telecomunicações, Lisbon, Portugal <sup>3</sup>Carnegie Mellon University, Pittsburgh, USA <sup>4</sup>Champalimaud Research, Lisbon, Portugal <sup>5</sup>TransPerfect, Lisbon, Portugal. Correspondence to: Saul Santos <saul.r.santos@tecnico.ulisboa.pt>.

attention-based in-context learning and variants of associative memories, including Hopfield networks (Ramsauer et al., 2020), fast weight programmers (Schlag et al., 2021), mesa-optimization (Von Oswald et al., 2023), and various forms of test-time regression and memory-based computation (Wang et al., 2025; Behrouz et al., 2024; Sun et al., 2025, *inter alia*). A key observation in several of these works is that standard softmax-based attention can be interpreted as *Gaussian kernel regression* on the key-value cache—this has motivated new transformer-related architectures such as *Memory Mosaics* (Zhang et al., 2025; Zhang & Bottou, 2025). However, *is the Gaussian kernel—and softmax attention—the best design choice?* It has been pointed out that the dense weights produced by softmax attention mechanisms may cause attention dispersion (Veličković et al., 2025)—a phenomenon where many weak contributions from irrelevant positions dilute the influence of truly relevant ones. Evidence from brain research (see §5 for details) suggests that neocortical memory retrieval is mediated by a relatively small set of well-separated memories, rather than weakly integrating over an increasingly large number of memories (Tulving, 2002; Gershman et al., 2025).

The observations above provide strong motivation for *sparse* attention alternatives, such as top- $k$  softmax (Gupta et al., 2021), sparsemax (Martins & Astudillo, 2016), and  $\alpha$ -entmax (Peters et al., 2019). The last two provide continuous, fully differentiable mappings from scores to attention weights while maintaining exact sparsity (Figure 1), enabling transformers to learn attention sparsity adaptively, rather than relying on a fixed truncation level. However, unlike the softmax case, a theoretical test-time regression understanding of sparse attention is currently missing.

Our work aims to fill that gap by providing a unified kernel regression perspective on both dense and sparse attention mechanisms. We show that a range of attention transformations—including softmax, sparsemax,  $\alpha$ -entmax, top- $k$  uniform, top- $k$  softmax, normalized ReLU, and a new transformation, ReLUmax—can be interpreted as Nadaraya-Watson estimators with different kernel functions. This viewpoint not only explains how sparsity naturally emerges from kernel design but also offers a principled framework for developing attention mechanisms with controlled spar-

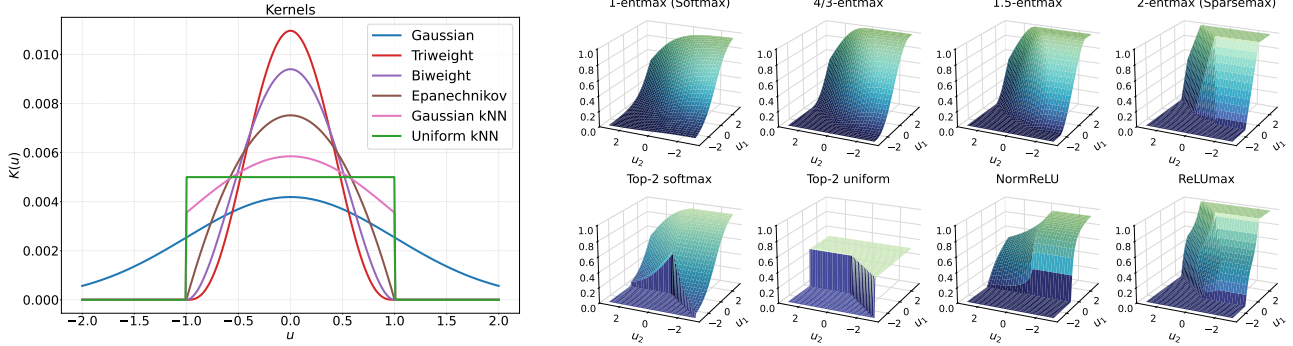


**Figure 1. Comparison between classical kernel functions and their corresponding attention activations.** The left plot shows normalized one-dimensional kernel functions commonly used in kernel regression evaluated on an input  $\mathbf{u} \in \mathbb{R}^n$ . The right panel shows different attention transformations applied to a 3D score vector  $\mathbf{u} = [0, u_1, u_2]$ . Each transformation allows an interpretation with corresponding kernels shown on the left: softmax ( $\alpha = 1$ ) corresponds to the Gaussian kernel; normalized ReLU, ReLUmax, and sparsemax ( $\alpha = 2$ ) are derived from Epanechnikov kernel variants ( $r = 1$ ); 4/3- and 1.5-entmax mirror biweight ( $r = 2$ ) and triweight ( $r = 3$ ) kernels; top- $k$  uniform mirrors the top- $k$  uniform kernel, while top- $k$  softmax can be viewed as a truncated Gaussian kernel.

sity. Our main contributions are: <sup>1</sup>

1. **We establish that sparsemax attention corresponds to auto-normalized Epanechnikov kernel regression** through an adaptive bandwidth, providing a rigorous link between sparse attention and compact support kernels.
2. **More generally, we show that  $\alpha$ -entmax attention with  $\alpha > 1$  corresponds to kernel regression with compact support kernels** of the form  $K(\mathbf{u}) \propto [1 - \|\mathbf{u}\|^2]_+^r$  where  $r = (\alpha - 1)^{-1}$ , encompassing widely used kernels such as Epanechnikov, biweight, and triweight.
3. **We unify top- $k$  and fixed-normalization sparse attention within the same kernel regression framework:** top- $k$  softmax corresponds to Gaussian kernel  $k$ -nearest-neighbor (kNN) regression, normalized ReLU corresponds to fixed-bandwidth Epanechnikov regression.
4. **We propose a new transformation, ReLUmax, which** corresponds to a max-anchored Epanechnikov variant.
5. **We conduct experiments demonstrating the benefits of compact kernels in Memory Mosaics**, a transformer-like architecture tied to kernel regression, achieving superior performance on simple language modeling, in-context learning, and length generalization tasks.

## 2. Background

### 2.1. Attention Mechanisms

The core of modern attention mechanisms is a transformation  $\pi : \mathbb{R}^n \rightarrow \Delta_n$  that maps a vector of scores to a probability distribution over the simplex  $\Delta_n := \{\mathbf{p} \in$

<sup>1</sup>Our code is available at [https://github.com/deepspin/sparse\\_att](https://github.com/deepspin/sparse_att).

$\mathbb{R}^n : \mathbf{p} \geq \mathbf{0}, \mathbf{1}^\top \mathbf{p} = 1\}$ . Given query  $\mathbf{q} \in \mathbb{R}^d$ , keys  $\mathbf{K} = [\mathbf{k}_1, \dots, \mathbf{k}_n]^\top \in \mathbb{R}^{n \times d}$ , and values  $\mathbf{V} = [\mathbf{v}_1, \dots, \mathbf{v}_n]^\top \in \mathbb{R}^{n \times d}$ , the attention mechanism computes

$$\sum_{i=1}^n \pi_i(\mathbf{K}\mathbf{q}) \mathbf{v}_i = \mathbf{V}^\top \pi(\mathbf{K}\mathbf{q}). \quad (1)$$

The choice of transformation  $\pi$  determines the behavior of the attention mechanism. The most common choice is the *softmax transformation*,  $\text{softmax}(\mathbf{z})_i = \frac{\exp(z_i)}{\sum_{j=1}^n \exp(z_j)}$ .

Softmax produces dense attention weights, with all positions receiving nonzero probabilities. For long contexts, this can lead to attention dispersion (Veličković et al., 2025) and makes token representations become less distinguishable (Barbero et al., 2024), motivating sparse alternatives.

### 2.2. Sparsemax and $\alpha$ -entmax

One such alternative is *sparsemax* (Martins & Astudillo, 2016), defined as the Euclidean projection onto the simplex,  $\text{sparsemax}(\mathbf{z}) := \arg \min_{\mathbf{p} \in \Delta_n} \frac{1}{2} \|\mathbf{z} - \mathbf{p}\|^2$ . The solution of this problem can be expressed as

$$\text{sparsemax}(\mathbf{z}) = [\mathbf{z} - \tau \mathbf{1}]_+, \quad (2)$$

where  $[x]_+ = \max(0, x)$  is the ReLU transformation and the threshold  $\tau$  is a normalizer ensuring  $\sum_i \max(z_i - \tau, 0) = 1$ .

The  $\alpha$ -entmax transformation (Peters et al., 2019) generalizes softmax and sparsemax by regularizing with the Tsallis  $\alpha$ -entropy (Tsallis, 1988),  $H_\alpha(\mathbf{p}) = \frac{1}{\alpha(\alpha-1)} (1 - \sum_i p_i^\alpha)$ :

$$\alpha\text{-entmax}(\mathbf{z}) := \arg \max_{\mathbf{p} \in \Delta_n} \mathbf{z}^\top \mathbf{p} + H_\alpha(\mathbf{p}). \quad (3)$$

The resulting solution takes the form

$$\alpha\text{-entmax}(\mathbf{z}) = [(\alpha - 1)\mathbf{z} - \tau \mathbf{1}]_+^{\frac{1}{\alpha-1}}, \quad (4)$$

where  $\tau$  is again a normalizer ensuring  $\sum_i p_i = 1$ . Sparsemax is recovered as the special case  $\alpha = 2$ , while the limit  $\alpha \rightarrow 1$  yields softmax. For  $\alpha > 1$ ,  $\alpha$ -entmax produces sparse probability distributions, with the sparsity level increasing as  $\alpha$  grows (see Figure 1).

### 2.3. Attention and Kernel Regression

Attention mechanisms can be interpreted through the lens of nonparametric kernel regression (Härdle, 1990; Tsybakov, 2008, §1.5). In this view, attention computes a locally weighted average of values, with the weights determined by a similarity-dependent kernel centered at the query.

Formally, given data points  $\{(\mathbf{k}_i, \mathbf{v}_i)\}_{i=1}^{n-1}$  and an input query  $\mathbf{q} \equiv \mathbf{k}_n$ , the *Nadaraya-Watson estimator* (Nadaraya, 1964; Watson, 1964) predicts the next target value as

$$\hat{\mathbf{v}}_n(\mathbf{q}) = \mathbb{E}[\mathbf{V}_n | \mathbf{q}] = \sum_{i=1}^{n-1} \frac{K_h(\mathbf{k}_i - \mathbf{q})}{\sum_{j=1}^{n-1} K_h(\mathbf{k}_j - \mathbf{q})} \mathbf{v}_i, \quad (5)$$

where  $K_h(\mathbf{u}) = \frac{1}{h^d} K\left(\frac{\mathbf{u}}{h}\right)$  is a kernel on  $\mathbb{R}^d$  with bandwidth  $h$ , and  $\int_{\mathbb{R}^d} K(\mathbf{u}) d\mathbf{u} = 1$ .<sup>2</sup> The kernel controls how strongly each data point  $(\mathbf{k}_i, \mathbf{v}_i)$  contributes to the prediction as a function of the distance between  $\mathbf{k}_i$  and the query  $\mathbf{q}$ .

**Softmax attention as Gaussian kernel regression.** Let  $\mathbf{K} = [\mathbf{k}_1, \dots, \mathbf{k}_{n-1}]^\top \in \mathbb{R}^{(n-1) \times d}$  denote the keys,  $\mathbf{q} \equiv \mathbf{k}_n$  denote the query, and  $\mathbf{V} = [\mathbf{v}_1, \dots, \mathbf{v}_n]^\top \in \mathbb{R}^{n \times d}$  the values. For clarity, we consider the setting in which the keys are  $\ell_2$ -normalized,  $\|\mathbf{q}\| = \|\mathbf{k}_i\| = 1$ , which allows us to directly relate dot-product attention to Euclidean distances.

Consider the Gaussian kernel  $K(\mathbf{u}) \propto \exp(-\frac{1}{2}\|\mathbf{u}\|^2)$ . Using the identity  $\frac{1}{2}\|\mathbf{k}_i - \mathbf{q}\|^2 = 1 - \mathbf{k}_i^\top \mathbf{q}$ , the Nadaraya-Watson estimator (5) yields

$$\hat{\mathbf{v}}_n(\mathbf{q}) = \sum_{i=1}^{n-1} \text{softmax}_i\left(\frac{\mathbf{K}\mathbf{q}}{h^2}\right) \mathbf{v}_i. \quad (6)$$

This expression recovers standard softmax attention, with the kernel bandwidth  $h$  corresponding to the *square root* of the softmax temperature. In transformers, the conventional scaling  $\mathbf{k}_i^\top \mathbf{q} / \sqrt{d}$  therefore corresponds to choosing  $h^2 = \sqrt{d}$ , i.e., an effective bandwidth  $h = d^{1/4}$ .

Choosing an appropriate bandwidth is central in kernel regression theory (Tsybakov, 2008). While vanilla transformers fix this choice via the  $\sqrt{d}$  scaling, recent works adapt the effective bandwidth as a function of the sequence length  $n$  to control attention dispersion and long-context behavior (Nakanishi, 2025; Vasylchenko et al., 2025; Zhang & Bottou, 2025). Furthermore, this kernel regression view sug-

<sup>2</sup>Throughout, we use “kernel” in the classical sense of kernel density estimation and kernel regression. This should not be confused with positive-definite kernels in the RKHS sense.

gests a natural generalization, raising the following question: “what if we use a different kernel than the Gaussian?”.

**Beyond Gaussian kernels.** Classical kernel regression is not restricted to Gaussian kernels. A wide range of kernels has been studied, differing in smoothness and support properties. Of particular interest are kernels with *compact support*, which assign zero weight to points beyond a certain distance and therefore induce locality and sparsity.

Common examples include the *Epanechnikov kernel*  $K(\mathbf{u}) \propto [1 - \|\mathbf{u}\|^2]_+$  (Epanechnikov, 1969), which has optimal properties in terms of minimizing mean integrated squared error (MISE), as well as its higher-order polynomial variants, including the *biweight*  $K(\mathbf{u}) \propto [1 - \|\mathbf{u}\|^2]_+^2$  and *triweight* kernels  $K(\mathbf{u}) \propto [1 - \|\mathbf{u}\|^2]_+^3$  (Scott, 2015). These kernels have restricted support to a bounded neighborhood around the query, as illustrated in Figure 1.

Another way to enforce compact support is to truncate the Gaussian kernel to the  $k$  nearest neighbors:

$$K_{\text{top-}k}(\mathbf{u}) \propto \begin{cases} \exp(-\frac{1}{2}\|\mathbf{u}\|^2/h^2), & \text{if } \|\mathbf{u}\| \leq \delta_{\max}, \\ 0, & \text{otherwise,} \end{cases} \quad (7)$$

where the threshold  $\delta_{\max}$  is implicitly determined by the set  $\mathcal{N}_k(\mathbf{q})$  of the  $k$  nearest neighbors of  $\mathbf{q}$  in feature space, i.e.,  $\|\mathbf{k}_i - \mathbf{q}\| \leq \delta_{\max}$  if and only if  $\mathbf{k}_i \in \mathcal{N}_k(\mathbf{q})$ . Similarly, a uniform kernel assigns equal weight to all points within a fixed radius:

$$K_{\text{uniform}}(\mathbf{u}) \propto \begin{cases} 1, & \text{if } \|\mathbf{u}\| \leq \delta_{\max}, \\ 0, & \text{otherwise.} \end{cases} \quad (8)$$

Epanechnikov, biweight, triweight, top- $k$  Gaussian, and uniform kernels are all examples of kernels with compact support. As we show in §3, these classical kernel choices give rise to different sparse attention mechanisms, providing a unified kernel-based perspective on locality and sparsity in attention. We illustrate these kernels in Figure 1.

### 2.4. Memory Mosaics

*Memory Mosaics* (Zhang et al., 2025) are networks of associative memories designed to perform prediction tasks using kernel regression. We base our work and experiments on this architecture as it explicitly implements a Nadaraya-Watson estimator as in (6), unlike vanilla transformers. That is, in Memory Mosaics, the query and key are *the same* by design, which aligns naturally with kernel regression:  $\mathbf{k}_n$  serves both as a query at the  $n^{\text{th}}$  time step to determine the weighting of past  $(n-1)$  stored values, and as a key at subsequent time steps.

Each memory unit contains a trainable feature extractor that

computes the keys and values from input vectors  $\mathbf{x}_i \in \mathbb{R}^{d_z}$ :

$$\begin{aligned} \text{Keys: } \mathbf{k}_n &= \varphi(\mathbf{x}_n, \mathbf{x}_{n-1}, \dots; \Theta), \\ \text{Values: } \mathbf{v}_n &= \psi(\mathbf{x}_{n+1}, \mathbf{x}_n, \mathbf{x}_{n-1}, \dots; \Theta), \end{aligned} \quad (9)$$

where  $\mathbf{k}_n, \mathbf{v}_n \in \mathbb{R}^d$ , and  $\Theta$  denotes learnable parameters. The key  $\mathbf{k}_n$  depends on current and past embeddings  $(\mathbf{x}_i)_{i \leq n}$ , while the value  $\mathbf{v}_n$  can access one step ahead to represent the feature the memory unit aims to predict. In practice, the projections include leaky averaging and normalization (Zhang et al., 2025):

$$\begin{aligned} \tilde{\mathbf{k}}_n &= W_\varphi \mathbf{z}_n, \quad \mathbf{k}_n = \text{Norm}(\tilde{\mathbf{k}}_n + \lambda_\varphi \bar{\mathbf{k}}_{n-1}), \\ \tilde{\mathbf{v}}_n &= W_\psi \mathbf{z}_n, \quad \mathbf{v}_n = \text{Norm}(\tilde{\mathbf{v}}_n + \lambda_\psi \tilde{\mathbf{v}}_{n+1}), \end{aligned} \quad (10)$$

where  $W_\varphi, W_\psi \in \mathbb{R}^{d \times d_z}$  are linear projections,  $\lambda_\varphi, \lambda_\psi$  are scalar leaky averaging coefficients, and  $\bar{\mathbf{k}}_{n-1}$  is the past averaged key. These keys and values are then used in the Nadaraya-Watson update (6) to form the contextual memory.

In the Memory Mosaics architecture, each standard transformer block is replaced by two parallel memories: a *contextual* memory unit, which applies attention via kernel regression using (6) and (10), and a *persistent* memory module. The persistent memory, inspired by earlier memory-augmented networks (Sukhbaatar et al., 2015), consists of learned memory slots that store information across sequences, providing a form of long-term associative memory. Conceptually, it functions similarly to self-attention over fixed memory slots and can replace a standard feed-forward network by offering additional capacity and nonlinear processing. The attention mechanism excludes the main diagonal, making use of (6) where the sum runs only up to  $n-1$  rather than  $n$ , which is why values can “peek” one step into the future in (10) to compensate. In this work, we focus on adapting the contextual memory unit to incorporate sparsity via different kernel choices while retaining the Nadaraya-Watson estimation principle.

### 3. Sparse Attention via Compact Kernels

We now formalize the connection between sparse attention mechanisms and kernel regression with compact support kernels. Starting from the kernel view of attention described in §2.3, we investigate how replacing the Gaussian kernel implicit in softmax attention with compact-support kernels naturally induces locality and sparsity.

**Normalized ReLU and Epanechnikov kernel.** Consider the Epanechnikov kernel mentioned earlier in §2.3, a compactly supported kernel widely used in kernel density estimation. Replacing the Gaussian kernel with the Epanechnikov

kernel, we can rewrite it in terms of the query  $\mathbf{q}$  as

$$K(\mathbf{k}_i - \mathbf{q}) = \left[ \frac{2}{h^2} \mathbf{k}_i^\top \mathbf{q} + \left(1 - \frac{2}{h^2}\right) \right]_+ = [\mathbf{k}_i^\top \mathbf{q} / \gamma + b]_+, \quad (11)$$

with  $\gamma = h^2/2$  and  $b = 1 - 2/h^2$ . Normalizing these ReLU-activated responses in (5) yields

$$\hat{\mathbf{v}}_n(\mathbf{q}) = \sum_{i=1}^{n-1} \frac{[\mathbf{k}_i^\top \mathbf{q} / \gamma + b]_+}{\sum_{j=1}^{n-1} [\mathbf{k}_j^\top \mathbf{q} / \gamma + b]_+} \mathbf{v}_i. \quad (12)$$

Thus, *normalized ReLU attention is equivalent to Epanechnikov kernel regression*, with sparsity arising from the ReLU truncation. This connection was also noted by Hoover et al. (2025), who used it to derive an Hopfield-like energy function. A limitation of the normalized ReLU (12) is that the attention weights are undefined when all pre-activations are negative, leading to  $\frac{0}{0}$ . Next, we show two principled ways to avoid this degeneracy: (i) *auto-normalization* (adaptive bandwidth) leading to sparsemax and  $\alpha$ -entmax, and (ii) *anchoring the support* at nearest keys, leading to ReLUMax.

#### 3.1. Auto-normalization (Adaptive Bandwidth)

An alternative to the normalization (12) is to choose a *data-dependent bandwidth*  $h$  which ensures the denominator in the Nadaraya-Watson estimator is a constant—we call this *auto-normalization*. We show next that this procedure yields attention transformations such as sparsemax and  $\alpha$ -entmax.

We begin with sparsemax and show how it arises from auto-normalized Epanechnikov regression. First, since we have normalized queries and keys, we can rewrite the squared distance as  $\frac{1}{2} \|\mathbf{k}_i - \mathbf{q}\|^2 = 1 - \mathbf{k}_i^\top \mathbf{q}$ . Then, introducing a temperature  $\gamma$ , the denominator in (5) can be rewritten as

$$\sum_{i=1}^{n-1} \left[ 1 - \frac{\|\mathbf{k}_i - \mathbf{q}\|^2}{h^2} \right]_+ = \frac{2\gamma}{h^2} \sum_{i=1}^{n-1} \left[ \frac{h^2}{2\gamma} - \frac{1}{\gamma} + \frac{\mathbf{k}_i^\top \mathbf{q}}{\gamma} \right]_+. \quad (13)$$

In Nadaraya-Watson estimation, the denominator has the effect of enforcing the weights to sum to one. An alternative is to absorb this normalization into the kernel scale. That is, rather than fixing  $h$ , we choose it so that the rectified responses sum to one:

$$\sum_{i=1}^{n-1} \left[ \frac{\mathbf{k}_i^\top \mathbf{q}}{\gamma} - \underbrace{\left( \frac{1}{\gamma} - \frac{h^2}{2\gamma} \right)}_{:=\tau} \right]_+ = 1. \quad (14)$$

With this choice, the denominator becomes a constant, and the normalized weights simply become the rectified responses. The normalizer  $\tau = \frac{1}{\gamma} - \frac{h^2}{2\gamma}$  coincides with the

sparsemax threshold in (2). As a result, by substituting (14) into (5), we obtain

$$\hat{v}_n(\mathbf{q}) = \sum_{i=1}^{n-1} \text{sparsemax}_i\left(\frac{\mathbf{K}\mathbf{q}}{\gamma}\right) \mathbf{v}_i, \quad (15)$$

showing that Epanechnikov kernel regression with auto-normalization is equivalent to sparsemax attention. In this construction the effective bandwidth is therefore *adaptive*  $h = \sqrt{2 - 2\gamma\tau}$ , where  $\tau$  (hence  $h$ ) is determined by the attention scores via (14), which depends only on the keys (but not the values). This contrasts with common bandwidth schedules that depend only on sequence length (Zhang & Bottou, 2025). It is also interesting to compare (15) with (6): in the softmax attention induced by the Gaussian kernel, we simply have  $h = \sqrt{\gamma}$ .

**From sparsemax to  $\alpha$ -entmax via compact kernels.** Instead of the linear truncation used by sparsemax,  $\alpha$ -entmax introduces a higher-order rectification controlled by a parameter  $\alpha > 1$ , yielding attention weights of the form (4) with the threshold  $\tau$  determined implicitly. On the kernel side, this corresponds to rectified polynomial kernels

$$K_h(\mathbf{u}) \propto \left[1 - \frac{\|\mathbf{u}\|^2}{h^2}\right]_+^r, \quad r = \frac{1}{\alpha - 1}, \quad (16)$$

recovering Epanechnikov ( $r = 1$ ), biweight ( $r = 2$ ), and triweight ( $r = 3$ ). Proposition 1 formalizes this correspondence, and the proof is given in Appendix A.

**Proposition 1.** Let  $r \geq 1$  and  $\alpha = 1 + \frac{1}{r}$ . Let  $\mathbf{K} = [\mathbf{k}_1, \dots, \mathbf{k}_{n-1}]^\top \in \mathbb{R}^{(n-1) \times d}$  be normalized keys,  $\mathbf{q} \equiv \mathbf{k}_n \in \mathbb{R}^d$  the query, and  $\mathbf{V} = [\mathbf{v}_1, \dots, \mathbf{v}_n]^\top$  the values. The  $\alpha$ -entmax attention with temperature  $\gamma$  satisfies

$$\sum_{i=1}^{n-1} \alpha\text{-entmax}_i\left(\frac{\mathbf{K}\mathbf{q}}{\gamma}\right) \mathbf{v}_i = \frac{\sum_{i=1}^{n-1} K_h(\mathbf{k}_i - \mathbf{q}) \mathbf{v}_i}{\sum_{i=1}^{n-1} K_h(\mathbf{k}_i - \mathbf{q})}, \quad (17)$$

where  $K_h(\mathbf{u}) \propto \left[1 - \frac{\|\mathbf{u}\|^2}{h^2}\right]_+^r$  and  $h$  is implicitly defined by  $h = \sqrt{2 - 2r\gamma\tau}$ .

Proposition 1 yields a continuous family of compact-support kernel attention mechanisms indexed by  $\alpha$ . In particular,  $r = 2$  corresponds to 1.5-entmax and the biweight kernel, while  $r = 3$  corresponds to  $\frac{4}{3}$ -entmax and the triweight kernel, recovering compact-kernel associative memories studied in Hopfield networks and related energy-based models (Wu et al., 2024; Santos et al., 2024; 2025). Figure 1 summarizes these correspondences between classical compact kernels and sparse attention transformations.

The rectified polynomial family is only one way to obtain compact support. A second, complementary route is to

*anchor* sparsity directly on the nearest keys by restricting attention to a neighborhood defined by kNN selection, i.e., by truncating an underlying kernel to a data-dependent support set. We turn to these anchored compact kernels next.

### 3.2. Anchored Compact Kernels

In this second route, instead of changing the kernel shape, we keep a base kernel and make its *support set* data-adaptive, either by truncation (top- $k$ ) or by max-anchoring (ReLUmax).

**Top- $k$  average pooling (uniform-kNN).** Consider the uniform kernel in (8). If we choose  $\delta_{\max}$  so that exactly  $k$  keys satisfy  $\|\mathbf{k}_i - \mathbf{q}\| \leq \delta_{\max}$ , then the support set is precisely the  $k$ -nearest-neighbor set  $\mathcal{N}_k(\mathbf{q})$ . Because all selected keys receive identical weight under the uniform kernel, the Nadaraya-Watson estimate reduces to

$$\hat{v}(\mathbf{q}) = \frac{1}{k} \sum_{i \in \mathcal{N}_k(\mathbf{q})} \mathbf{v}_i. \quad (18)$$

Thus, top- $k$  average pooling is equivalent to uniform-kNN kernel regression with an adaptively chosen radius that admits exactly  $k$  neighbors.

**Top- $k$  softmax (truncated Gaussian).** A smoother, anchored alternative is to use a Gaussian kernel within the  $k$ -nearest-neighbor set and set all weights to zero outside it. This corresponds to the truncated kernel in (7). Normalizing these weights yields

$$\hat{v}(\mathbf{q}) = \sum_{i \in \mathcal{N}_k(\mathbf{q})} \frac{K_{\text{top-}k}(\mathbf{k}_i - \mathbf{q})}{\sum_{j \in \mathcal{N}_k(\mathbf{q})} K_{\text{top-}k}(\mathbf{k}_j - \mathbf{q})} \mathbf{v}_i. \quad (19)$$

This mechanism can be interpreted as Gaussian kernel regression with a data-adaptive compact support set, given by  $\mathcal{N}_k(\mathbf{q})$ , yielding a sparse kNN-style attention mechanism (Gupta et al., 2021).

**ReLUmax.** The top- $k$  constructions above enforce compact support by *hard* truncation via kNN selection. We consider a new transformation, ReLUmax, which anchors support *softly* at the best-matching key while retaining a compact kernel and avoiding the empty-support degeneracy of normalized ReLU. Let  $m := \max_j \mathbf{k}_j^\top \mathbf{q}$  and  $b > 0 \in \mathbb{R}$  be a hyperparameter. The ReLUmax kernel is given by

$$K_{\text{relu max}}(\mathbf{k}_i - \mathbf{q}) \propto \left[b + \frac{\mathbf{k}_i^\top \mathbf{q} - m}{h^2}\right]_+. \quad (20)$$

The corresponding Nadaraya-Watson estimate is obtained by normalizing these weights:

$$\hat{v}(\mathbf{q}) = \sum_{i=1}^{n-1} \frac{\left[\frac{\mathbf{k}_i^\top \mathbf{q} - m}{h^2} + b\right]_+}{\sum_{k=1}^{n-1} \left[\frac{\mathbf{k}_k^\top \mathbf{q} - m}{h^2} + b\right]_+} \mathbf{v}_i. \quad (21)$$

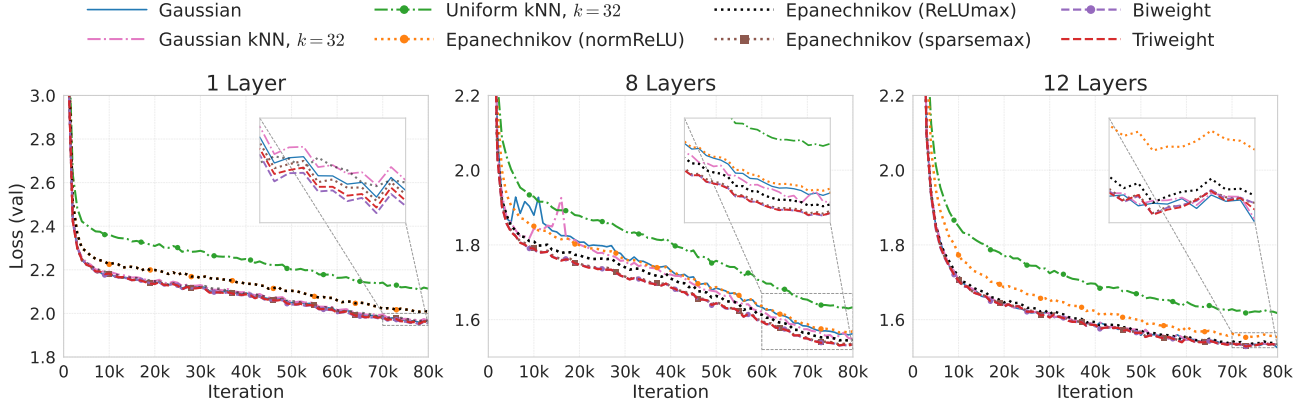


Figure 2. Validation loss of Memory Mosaic models with different kernels. Comparison on the BabiStories dataset for varying model depths. The horizontal axis shows the number of training iterations.

Importantly, since  $b > 0$ , in the worst case where all attention scores equal  $m$ , at least one rectified score will be strictly positive, and so the denominator in (21) cannot be zero. Hence, ReLUMax avoids the 0/0 degeneracy of normalized ReLU (12) while preserving compact support. Furthermore, we note that (21) yields an explicit characterization of the active set:

$$\begin{aligned} K_{\text{relumax}}(\mathbf{k}_i - \mathbf{q}) > 0 &\iff b + \frac{\mathbf{k}_i^\top \mathbf{q} - m}{h^2} > 0 \\ &\iff \mathbf{k}_i^\top \mathbf{q} > m - bh^2. \end{aligned} \quad (22)$$

Thus, ReLUMax selects *all keys within a fixed similarity margin of the maximum similarity*. This is fundamentally different from top- $k$  since the number of active keys adapts to the distribution of score gaps rather than being fixed. In fact, this points to a *top- $p$*  viewpoint. Top- $k$  fixes the *cardinality* of the support, whereas ReLUMax fixes a *margin-to-maximum* threshold, with keys being kept whenever their score exceeds  $m - bh^2$ . Consequently, the retained set expands when many keys have scores close to the maximum (small gaps) and shrinks when the maximum is well separated (large gaps). In this sense, ReLUMax behaves like a continuous analogue of nucleus selection as it adaptively includes “as many keys as needed” near the top of the score distribution, but does so via a smooth, differentiable margin.

## 4. Experiments

We conduct three sets of experiments to validate our theoretical findings and demonstrate the practical benefits of our kernel-based attention mechanisms.

### 4.1. Language Modeling

**Setup.** We replicate Memory Mosaics (Zhang et al., 2025) with our proposed kernel-based sparse attention mechanisms and conduct language modeling experiments on small, self-

contained narratives written in simple English, designed to be comprehensible to a young child. Specifically, we follow the methodology of Li & Eldan (2024) and Zhang et al. (2025), and evaluate on BabiStories. To study the effect of different attention mechanisms, we replace the standard softmax attention used in Memory Mosaics (Zhang et al., 2025) with the family of kernel-based methods described in §3. Namely, we consider Gaussian (softmax) attention and compact rectified polynomial kernels: Epanechnikov ( $r=1$ ) via normalized ReLU, sparsemax, and ReLUMax ( $b=1$ ), and higher-order biweight ( $r=2$ ) and triweight ( $r=3$ ), which correspond to  $\alpha$ -entmax with  $\alpha=1.5$  and  $\alpha=\frac{4}{3}$ , respectively. In addition to  $r$ -order rectified polynomial kernels, we evaluate discrete uniform and Gaussian kNN attention. Further experimental details can be found in §B.1.

**Discussion.** Figure 2 shows a comparison of models equipped with different kernel-based attention mechanisms across model depths in terms of validation loss. For shallow models (one layer), compactly supported kernels—Epanechnikov, biweight, and triweight—achieve lower validation loss than dense Gaussian attention and top- $k$  baselines. As depth increases to 8 layers, this advantage remains, and rectified polynomial kernels outperform dense softmax attention and anchored top- $k$  variants across iterations. With 12 layers, the gap is narrower and, with the exception of normReLU and uniform kNN, all approaches achieve roughly the same validation loss. Interestingly, while top- $k$  Gaussian attention can reach competitive validation loss at intermediate depths, it exhibits mild instability, likely due to the non-smoothness introduced by discrete neighbor selection. Among sparse mechanisms, auto-normalized attention mappings—corresponding to sparsemax and  $\alpha$ -entmax—consistently perform better than normReLU, which has a fixed rather than adaptive bandwidth. Finally, while ReLUMax outperforms normReLU with 8 and 12 layers, it slightly underperforms adaptive normalization methods.

**Table 1. Performance comparison across varying training set sizes in the Regbench in-context learning benchmark.** Accuracy ( $\uparrow$ ) measures the correct prediction rate, and TVD ( $\downarrow$ ) measures divergence from the target distribution. We **bold** the best performing models.

Method	1k		2.5k		5k		10k		20k		40k	
	Acc $\uparrow$	TVD $\downarrow$										
RetNet	51.3	67.4	50.5	63.9	81.5	33.3	88.4	25.7	90.8	22.5	92.6	18.9
H3	51.5	65.1	58.0	57.0	70.9	47.4	76.9	41.4	80.7	36.3	87.7	25.4
Gla	51.8	65.3	51.1	62.2	82.1	31.0	90.2	24.5	91.2	21.2	92.9	19.0
S4	52.1	62.8	51.7	62.2	54.5	59.0	63.3	52.9	72.1	45.8	82.5	33.8
Mamba	69.4	51.0	79.4	41.0	88.7	30.6	90.5	28.4	91.3	27.0	91.5	27.0
Transformer	54.5	62.6	92.4	20.5	92.7	18.9	94.8	15.7	95.1	15.0	95.5	13.9
<b>Memory Mosaics:</b>												
Gaussian	93.9	34.1	93.7	20.8	94.6	17.7	95.0	15.9	<b>95.4</b>	15.3	95.4	14.2
Gaussian kNN, $k = 16$	93.4	33.3	93.7	19.8	94.4	17.2	94.8	16.0	94.8	16.0	95.0	14.9
Uniform kNN, $k = 16$	84.6	41.1	85.6	28.3	86.1	27.2	86.2	26.4	86.5	26.4	86.4	26.4
Epanechnikov (normReLU)	84.3	43.6	87.0	29.6	90.1	24.6	91.6	21.7	93.1	19.4	93.3	18.6
Epanechnikov (ReLUmax)	93.8	36.8	94.2	20.4	94.3	17.8	94.9	<b>15.7</b>	<b>95.4</b>	<b>15.0</b>	95.4	14.1
Epanechnikov (sparsemax)	<b>94.2</b>	<b>32.5</b>	94.0	19.3	94.4	17.1	94.9	15.9	95.0	<b>15.0</b>	95.4	14.0
Biweight	93.8	33.0	<b>94.3</b>	19.2	94.7	16.6	<b>95.2</b>	<b>15.7</b>	95.0	15.8	<b>95.5</b>	<b>13.8</b>
Triweight	93.9	32.9	<b>94.3</b>	<b>19.0</b>	<b>94.8</b>	<b>16.2</b>	94.9	16.1	95.1	15.3	95.3	14.4

## 4.2. In-Context Learning

**Setup.** We also evaluate our models on an in-context learning task. To rigorously compare the in-context learning capabilities of different architectures, we adopt the RegBench benchmark (Akyürek et al., 2024), a diagnostic suite designed to probe sequence models’ ability to infer the generative processes of regular languages, which constructs random artificial languages defined by a PFA with sequences consisting of 10 to 20 strings sampled from the same PFA. We compare baseline transformers and kernelized variants of our sparse Memory Mosaic architectures, as well as several established baselines including S4 (Gu et al., 2022), Gla (Yang et al., 2023), RetNet (Sun et al., 2023), H3 (Fu et al., 2023), Mamba (Gu & Dao, 2023), and standard transformers (Vaswani et al., 2017). Our models match the sequence length and vocabulary size of Akyürek et al. (2024) and follow the same hyperparameter tuning strategy. Full experimental details are provided in §B.2. Each model is trained on datasets ranging from 1k to 40k examples and evaluated using per-token loss as a function of the generated token position for a test set of 1k examples.

**Discussion.** Table 1 compares models on RegBench using last-token accuracy and total variation distance (TVD). Among the Memory Mosaic variants, rectified polynomial kernels (Triweight, Biweight, and Epanechnikov) consistently match or slightly outperform the Gaussian kernel in the low-data regime (1k–5k), achieving both higher accuracy and lower TVD. As the dataset size increases, performance differences narrow, with all compact kernels converging to similar accuracy (around 95%) and TVD. Within the Epanechnikov family, sparsemax performs best overall, fol-

lowed closely by ReLUmax in terms of accuracy and TVD. In contrast, normalized ReLU shows a clear degradation in both metrics, suggesting that simple thresholded normalization without adaptive support selection is insufficient in this setting. Fixed top- $k$  uniform attention underperforms across all data scales, highlighting the limitations of hard, data-independent sparsity compared to kernel-based adaptive weighting. Overall, these results indicate that adaptive sparsity induced by compact kernels is most beneficial in data-scarce regimes.

## 4.3. Length Generalization

**Setup.** We evaluate the length generalization capabilities of our Memory Mosaics using synthetic tasks, following the setup of Vasylenko et al. (2025), such as MQMTAR (multi-query multi-token associative recall), sequence sorting, and reversing, which provide precise control over training and test sequence lengths. These tasks test the model’s ability to maintain attention on relevant, sparse subsets of tokens, and probe the model’s ability to learn an underlying length-agnostic algorithm, rather than memorizing patterns. Full experimental details are provided in §B.3.

**Discussion.** The results in Table 2 show that Gaussian attention performs well in-distribution but quickly deteriorates when extrapolating to long sequences. Top- $k$  uniform attention is too crude, failing to extrapolate for any of the tasks. Gaussian kNN mitigates some degradation by limiting attention to nearest neighbors, yet it still achieves poor length extrapolation, especially on very long sequences. In contrast, our rectified polynomial kernels exhibit strong and stable generalization, particularly on the MQMTAR task.

Table 2. Exact match accuracy on representative synthetic tasks. In-distribution results ( $n = 64$ ) and out-of-distribution performance at increasing sequence lengths are reported. Values show the mean across three seeds, with the maximum across seeds indicated in superscript. Best average performance is in **bold** and overall maximum performance is underlined.  $L$  represents the number of layers.

Kernel	MQMTAR ( $L = 4$ )						Reverse ( $L = 4$ )		Sort ( $L = 2$ )			
	1×	2×	4×	8×	16×	32×	64×	1×	1.5×	1×	2×	4×
Gaussian	0.99 <sup>(1.00)</sup>	0.96 <sup>(1.00)</sup>	0.93 <sup>(0.99)</sup>	0.85 <sup>(0.97)</sup>	0.64 <sup>(0.81)</sup>	0.14 <sup>(0.20)</sup>	0.00 <sup>(0.00)</sup>	<b>1.00</b> <sup>(1.00)</sup>	0.14 <sup>(0.38)</sup>	<b>1.00</b> <sup>(1.00)</sup>	0.06 <sup>(0.17)</sup>	0.00 <sup>(0.00)</sup>
Gaussian kNN, $k = 32$	0.99 <sup>(1.00)</sup>	0.97 <sup>(1.00)</sup>	0.93 <sup>(0.99)</sup>	0.84 <sup>(0.96)</sup>	0.68 <sup>(0.85)</sup>	0.27 <sup>(0.36)</sup>	0.05 <sup>(0.05)</sup>	0.99 <sup>(1.00)</sup>	0.00 <sup>(0.00)</sup>	<b>1.00</b> <sup>(1.00)</sup>	0.80 <sup>(0.91)</sup>	0.01 <sup>(0.02)</sup>
Uniform kNN, $k = 32$	0.04 <sup>(0.08)</sup>	0.00 <sup>(0.00)</sup>	0.42 <sup>(0.66)</sup>	0.00 <sup>(0.00)</sup>	<b>1.00</b> <sup>(1.00)</sup>	0.00 <sup>(0.00)</sup>	0.00 <sup>(0.00)</sup>					
Epanechnikov (normReLU)	<b>1.00</b> <sup>(1.00)</sup>	<b>1.00</b> <sup>(1.00)</sup>	0.89 <sup>(1.00)</sup>	0.66 <sup>(1.00)</sup>	0.44 <sup>(1.00)</sup>	0.33 <sup>(0.98)</sup>	<b>0.31</b> <sup>(0.94)</sup>	<b>1.00</b> <sup>(1.00)</sup>	0.19 <sup>(0.56)</sup>	<b>1.00</b> <sup>(1.00)</sup>	0.05 <sup>(0.14)</sup>	0.00 <sup>(0.00)</sup>
Epanechnikov (ReLUmax)	<b>1.00</b> <sup>(1.00)</sup>	<b>1.00</b> <sup>(1.00)</sup>	0.99 <sup>(1.00)</sup>	0.92 <sup>(0.96)</sup>	0.74 <sup>(0.87)</sup>	0.42 <sup>(0.59)</sup>	0.12 <sup>(0.18)</sup>	<b>1.00</b> <sup>(1.00)</sup>	0.23 <sup>(0.68)</sup>	<b>1.00</b> <sup>(1.00)</sup>	0.80 <sup>(1.00)</sup>	<b>0.30</b> <sup>(0.91)</sup>
Epanechnikov (sparsemax)	<b>1.00</b> <sup>(1.00)</sup>	<b>1.00</b> <sup>(1.00)</sup>	<b>1.00</b> <sup>(1.00)</sup>	<b>0.98</b> <sup>(1.00)</sup>	0.86 <sup>(0.98)</sup>	<b>0.63</b> <sup>(0.84)</sup>	<b>0.31</b> <sup>(0.51)</sup>	<b>1.00</b> <sup>(1.00)</sup>	0.03 <sup>(0.06)</sup>	<b>1.00</b> <sup>(1.00)</sup>	0.92 <sup>(1.00)</sup>	0.29 <sup>(0.79)</sup>
Biweight	<b>1.00</b> <sup>(1.00)</sup>	<b>1.00</b> <sup>(1.00)</sup>	0.99 <sup>(1.00)</sup>	0.95 <sup>(0.99)</sup>	0.75 <sup>(0.93)</sup>	0.51 <sup>(0.74)</sup>	0.23 <sup>(0.42)</sup>	<b>1.00</b> <sup>(1.00)</sup>	0.05 <sup>(0.06)</sup>	<b>1.00</b> <sup>(1.00)</sup>	0.39 <sup>(1.00)</sup>	0.26 <sup>(0.77)</sup>
Triweight	<b>1.00</b> <sup>(1.00)</sup>	<b>1.00</b> <sup>(1.00)</sup>	0.99 <sup>(1.00)</sup>	0.97 <sup>(0.98)</sup>	<b>0.89</b> <sup>(0.95)</sup>	0.61 <sup>(0.76)</sup>	0.25 <sup>(0.45)</sup>	<b>1.00</b> <sup>(1.00)</sup>	<b>0.26</b> <sup>(0.70)</sup>	<b>1.00</b> <sup>(1.00)</sup>	<b>0.98</b> <sup>(0.99)</sup>	0.07 <sup>(0.11)</sup>

Triweight and biweight kernels outperform Gaussian and top- $k$  mechanisms on MQMTAR, with triweight also leading on the reverse task, while preserving high accuracy over longer sequences. Epanechnikov-based attention mechanisms, specifically ReLUmax and sparsemax, consistently achieve perfect in-distribution accuracy while maintaining superior length extrapolation performance, with sparsemax showing better generalization performance. Finally, ReLUmax outperforms normReLU, benefitting from its max-anchoring operation, with improved stability at longer sequence lengths.

## 5. Discussion and Related Work

**Sparse attention mechanisms.** Sparse attention offers an alternative to dense softmax, enabling models to focus on a subset of relevant tokens. Early approaches such as top- $k$  softmax (Gupta et al., 2021) enforced sparsity by keeping only the largest attention scores, but suffered from non-smooth gradients and a fixed attention budget. One line of work employs predefined sparse patterns, such as local sliding windows or fixed strides, such as LongFormer (Beltagy et al., 2020) and BigBird (Zaheer et al., 2020). Other methods introduce end-to-end learnable sparsity by replacing softmax with differentiable alternatives such as sparsemax (Martins & Astudillo, 2016) and its generalization  $\alpha$ -entmax (Peters et al., 2019). More recently, Hu et al. (2023), Wu et al. (2024), Santos et al. (2024; 2025), and Hoover et al. (2025) develop sparse Hopfield networks—mathematically equivalent to sparse attention mechanisms—, while Vasylenko et al. (2025) show that  $\alpha$ -entmax attention can mitigate attention dispersion and representational collapse for long sequences. Our paper provides a test-time regression interpretation of these frameworks.

**Kernel methods in transformers.** Early interpretations view softmax attention as a kind of similarity kernel, where attention weights arise from pairwise comparisons between queries and keys (Tsai et al., 2019). Building on this statistical view, recent work has shown that at test time transform-

ers can behave like implicit Nadaraya-Watson estimators, with attention patterns converging to regression-like weights that resemble classical kernel regression outputs (Wang et al., 2025). Related research explores test-time regression and meta-learning behaviours in transformers and fast weight systems where models implicitly solve regression or optimization tasks in context (Von Oswald et al., 2023; Schlag et al., 2021; Behrouz et al., 2024; Sun et al., 2025). While prior work focuses on dense kernels and efficient approximations, we extend the kernel regression view to sparse, compactly supported kernels, unifying dense and sparse attention within a single framework.

**Neurobiological context.** In the domain of neurobiological systems such as humans, the problem of understanding the long-range dependency structure in sequences arises in episodic memory (Tulving, 2002). The hippocampal indexing theory suggests that the brain solves this problem with hippocampal engrams serving as indices with which the brain retrieves neocortical traces of previous experiences (Teyler & DiScenna, 1986; Goode et al., 2020). Notably, a core characteristic of hippocampal population activity is sparseness. This property of hippocampal activity is often attributed to its functional role of pattern separation (Yassa & Stark, 2011). From the perspective of the current work, hippocampal indices serve as keys, which can be queried, to neocortical values (Gershman et al., 2025). Thus, sparsity can be understood as an implicit use of compact-support kernels whereby neocortical memory retrieval is mediated by a relatively small set of well-separated memories, rather than weakly integrating over an increasingly large number of memories accumulated over a lifetime (Tulving, 2002).

## 6. Conclusions

In this work, we show that sparse attention mechanisms can be interpreted as kernel regression with compactly supported kernels, providing a principled framework that unifies dense and sparse attention. We demonstrate that  $r$ -order rectified polynomial kernels allow controlled sparsity, from which

several attention mechanisms—including  $\alpha$ -entmax—can be derived. For  $r = 1$ , the Epanechnikov kernel underlies several attention mechanisms: normalized ReLU, which can produce empty-support indeterminacies when all pre-activations are negative; ReLUMax, which anchors the support at the maximum key to avoid this issue; and sparsemax, which further introduces adaptive normalization by adjusting the kernel bandwidth based on the attention scores also ensuring non-degenerate attention. Our empirical results confirm that attention mechanisms with adaptive normalization outperform dense Gaussian and heuristic top- $k$  methods, generally delivering superior performance.

## Impact Statement

This work advances the understanding of sparse attention mechanisms by framing them as kernel regression with compactly supported kernels. While we do not foresee ethical complications as a direct result of our method, we note that our contributions can be applied for training language models, and thus they inherit the broader ethical considerations associated with transformer-based language models. We emphasize responsible deployment, careful dataset curation, and energy-efficient training practices in such cases.

## Acknowledgments

We would like to thank Hugo Pitorro, Lili Mou, Pavlo Vasylenko, Mathias Lindemann, and the SARDINE lab team for the helpful discussions. We thank the Champalimaud Foundation for supporting this research. This work was supported by the project DECOLLAGE (ERC-2022-CoG 101088763), by the Portuguese Recovery and Resilience Plan through project C645008882-00000055 (Center for Responsible AI), and by FCT/MECI through national funds and when applicable co-funded EU funds under UID/50008: Instituto de Telecomunicações.

## References

Akyürek, E., Wang, B., Kim, Y., and Andreas, J. In-context language learning: Architectures and algorithms, 2024. URL <https://arxiv.org/abs/2401.12973>.

Barbero, F., Banino, A., Kapturowski, S., Kumaran, D., Madeira Araújo, J., Vitvitskyi, O., Pascanu, R., and Veličković, P. Transformers need glasses! information over-squashing in language tasks. *Advances in Neural Information Processing Systems*, 37:98111–98142, 2024.

Behrouz, A., Zhong, P., and Mirrokni, V. Titans: Learning to memorize at test time. *arXiv preprint arXiv:2501.00663*, 2024.

Beltagy, I., Peters, M. E., and Cohan, A. Longformer: The Long-Document Transformer. *arXiv:2004.05150 [cs]*, April 2020. URL <http://arxiv.org/abs/2004.05150>. arXiv: 2004.05150.

Epanechnikov, V. A. Non-parametric estimation of a multivariate probability density. *Theory of Probability & Its Applications*, 14(1):153–158, 1969. doi: 10.1137/1114019. URL <https://doi.org/10.1137/1114019>.

Fu, D. Y., Dao, T., Saab, K. K., Thomas, A. W., Rudra, A., and Ré, C. Hungry Hungry Hippos: Towards language modeling with state space models. In *International Conference on Learning Representations*, 2023.

Gershman, S. J., Fiete, I., and Irie, K. Key-value memory in the brain. *arXiv:2501.02950 [q-bio.NC]*, 2025. URL <https://arxiv.org/abs/2501.02950>. Preprint, Jan 2025.

Gonçalves, N., Treviso, M. V., and Martins, A. Adasplash: Adaptive sparse flash attention. In *Forty-second International Conference on Machine Learning*, 2025. URL <https://openreview.net/forum?id=OWIPDWhUc0>.

Goode, T. D., Tanaka, K. Z., Sahay, A., and McHugh, T. J. An integrated index: Engrams, place cells, and hippocampal memory. *Neuron*, 107(5):805–820, 2020. doi: 10.1016/j.neuron.2020.07.011. Epub 2020 Aug 6.

Gu, A. and Dao, T. Mamba: Linear-time sequence modeling with selective state spaces. *arXiv preprint arXiv:2312.00752*, 2023.

Gu, A., Goel, K., and Ré, C. Efficiently modeling long sequences with structured state spaces. In *The International Conference on Learning Representations (ICLR)*, 2022.

Gupta, A., Dar, G., Goodman, S., Ciprut, D., and Beiran, J. Memory-efficient transformers via top-k attention. In Moosavi, N. S., Gurevych, I., Fan, A., Wolf, T., Hou, Y., Marasović, A., and Ravi, S. (eds.), *Proceedings of the Second Workshop on Simple and Efficient Natural Language Processing*, pp. 39–52, Virtual, November 2021. Association for Computational Linguistics. doi: 10.18653/v1/2021.sustainlp-1.5. URL <https://aclanthology.org/2021.sustainlp-1.5/>.

Härdle, W. *Applied nonparametric regression*. Number 19. Cambridge university press, 1990.

Hoover, B., Balasubramanian, K., Krotov, D., and Ram, P. Dense associative memory with epanechnikov energy. In *New Frontiers in Associative Memories*, 2025.

Hu, J. Y.-C., Yang, D., Wu, D., Xu, C., Chen, B.-Y., and Liu, H. On sparse modern hopfield model. *Advances in Neural Information Processing Systems*, 36:27594–27608, 2023.

Li, Y. and Eldan, R. Tinystories: How small can language models be and still speak coherent english, 2024. URL <https://openreview.net/forum?id=yiPtWSrBrN>.

Martins, A. and Astudillo, R. From softmax to sparsemax: A sparse model of attention and multi-label classification. In Balcan, M. F. and Weinberger, K. Q. (eds.), *International Conference on Machine Learning (ICML)*, volume 48 of *Proceedings of Machine Learning Research*, pp. 1614–1623, New York, New York, USA, 20–22 Jun 2016. PMLR. URL <http://proceedings.mlr.press/v48/martins16.html>.

Nadaraya, E. A. On estimating regression. *Theory of Probability & Its Applications*, 9(1):141–142, 1964. doi: 10.1137/1109020. URL <https://doi.org/10.1137/1109020>.

Nakanishi, K. M. Scalable-softmax is superior for attention. *arXiv preprint arXiv:2501.19399*, 2025.

Peters, B., Niculae, V., and Martins, A. F. Sparse sequence-to-sequence models. In *Proceedings of the 57th Annual Meeting of the Association for Computational Linguistics*, pp. 1504–1519, 2019.

Radford, A., Wu, J., Child, R., Luan, D., Amodei, D., and Sutskever, I. Language models are unsupervised multitask learners. 2019.

Ramsauer, H., Schäfl, B., Lehner, J., Seidl, P., Widrich, M., Gruber, L., Holzleitner, M., Adler, T., Kreil, D., Kopp, M. K., et al. Hopfield networks is all you need. In *International Conference on Learning Representations*, 2020.

Santos, S., Niculae, V., McNamee, D., and Martins, A. F. Hopfield-fenchel-young networks: A unified framework for associative memory retrieval. *Journal of Machine Learning Research*, 26(265):1–51, 2025. URL <http://jmlr.org/papers/v26/24-1961.html>.

Santos, S. J. R., Niculae, V., McNamee, D. C., and Martins, A. Sparse and structured hopfield networks. In *Forty-first International Conference on Machine Learning*, 2024.

Schlag, I., Irie, K., and Schmidhuber, J. Linear transformers are secretly fast weight programmers. In *International conference on machine learning*, pp. 9355–9366. PMLR, 2021.

Scott, D. W. *Multivariate density estimation: theory, practice, and visualization*. John Wiley & Sons, 2015.

Sukhbaatar, S., szlam, a., Weston, J., and Fergus, R. End-to-end memory networks. In Cortes, C., Lawrence, N., Lee, D., Sugiyama, M., and Garnett, R. (eds.), *Advances in Neural Information Processing Systems*, volume 28. Curran Associates, Inc., 2015. URL [https://proceedings.neurips.cc/paper\\_files/paper/2015/file/8fb21ee7a2207526da55a679f0332de2-Paper.pdf](https://proceedings.neurips.cc/paper_files/paper/2015/file/8fb21ee7a2207526da55a679f0332de2-Paper.pdf).

Sun, Y., Dong, L., Huang, S., Ma, S., Xia, Y., Xue, J., Wang, J., and Wei, F. Retentive network: A successor to transformer for large language models, 2023.

Sun, Y., Li, X., Dalal, K., Xu, J., Vikram, A., Zhang, G., Dubois, Y., Chen, X., Wang, X., Koyejo, S., et al. Learning to (learn at test time): Rnns with expressive hidden states. In *Forty-second International Conference on Machine Learning*, 2025.

Teyler, T. J. and DiScenna, P. The hippocampal memory indexing theory. *Behavioral Neuroscience*, 100(2):147–154, 1986. doi: 10.1037/0735-7044.100.2.147.

Tsai, Y.-H. H., Bai, S., Yamada, M., Morency, L.-P., and Salakhutdinov, R. Transformer dissection: An unified understanding for transformer’s attention via the lens of kernel. In *EMNLP*, 2019.

Tsallis, C. Possible generalization of boltzmann-gibbs statistics. *Journal of statistical physics*, 52:479–487, 1988.

Tsybakov, A. B. Nonparametric estimators. In *Introduction to Nonparametric Estimation*, pp. 1–76. Springer, 2008.

Tulving, E. Episodic memory: From mind to brain. *Annual Review of Psychology*, 53:1–25, 2002. doi: 10.1146/annurev.psych.53.100901.135114.

Vaswani, A., Shazeer, N., Parmar, N., Uszkoreit, J., Jones, L., Gomez, A. N., Kaiser, Ł., and Polosukhin, I. Attention is all you need. *Advances in neural information processing systems*, 30, 2017. URL <https://papers.nips.cc/paper/2017/hash/3f5ee243547dee91fb053c1c4a845aa-Abstract.html>.

Vasylenko, P., Pitorro, H., Martins, A. F. T., and Treviso, M. Long-context generalization with sparse attention, 2025. URL <https://arxiv.org/abs/2506.16640>.

Veličković, P., Perivolaropoulos, C., Barbero, F., and Pascanu, R. Softmax is not enough (for sharp size generalisation). In *Forty-second International Conference on Machine Learning*, 2025. URL <https://openreview.net/forum?id=S4JmmpnSPy>.

Von Oswald, J., Niklasson, E., Randazzo, E., Sacramento, J., Mordvintsev, A., Zhmoginov, A., and Vladymyrov, M. Transformers learn in-context by gradient descent. In *International Conference on Machine Learning*, pp. 35151–35174. PMLR, 2023.

Wang, K. A., Shi, J., and Fox, E. B. Test-time regression: a unifying framework for designing sequence models with associative memory, 2025. URL <https://arxiv.org/abs/2501.12352>.

Watson, G. S. Smooth regression analysis. *Sankhyā: The Indian Journal of Statistics, Series A* (1961-2002), 26(4): 359–372, 1964. ISSN 0581572X. URL <http://www.jstor.org/stable/25049340>.

Wu, D., Hu, J. Y.-C., Li, W., Chen, B.-Y., and Liu, H. Stanhop: Sparse tandem hopfield model for memory-enhanced time series prediction. In *The Twelfth International Conference on Learning Representations*, 2024.

Yang, S., Wang, B., Shen, Y., Panda, R., and Kim, Y. Gated linear attention transformers with hardware-efficient training. *arXiv preprint arXiv:2312.06635*, 2023. URL <https://arxiv.org/abs/2312.06635>.

Yassa, M. A. and Stark, C. E. L. Pattern separation in the hippocampus. *Trends in Neurosciences*, 34(10):515–525, 2011. doi: 10.1016/j.tins.2011.06.006.

Zaheer, M., Guruganesh, G., Dubey, K. A., Ainslie, J., Alberti, C., Ontanon, S., Pham, P., Ravula, A., Wang, Q., Yang, L., et al. Big bird: Transformers for longer sequences. *Advances in Neural Information Processing Systems*, 33, 2020.

Zhang, J. and Bottou, L. Memory mosaics at scale. In *Advances in Neural Information Processing Systems*, 2025.

Zhang, J., Nolte, N., Sadhukhan, R., Chen, B., and Bottou, L. Memory mosaics. In Yue, Y., Garg, A., Peng, N., Sha, F., and Yu, R. (eds.), *International Conference on Representation Learning*, volume 2025, pp. 36412–36433, 2025. URL [https://proceedings iclr.cc/paper\\_files/paper/2025/file/59c3ac496e6fe7be0c2c2b95014e2210-Paper-Conference.pdf](https://proceedings iclr.cc/paper_files/paper/2025/file/59c3ac496e6fe7be0c2c2b95014e2210-Paper-Conference.pdf).

## A. Proof of Proposition 1

*Proof.* Let  $\mathbf{q} \equiv \mathbf{k}_n$  and  $r = \frac{1}{\alpha-1}$ . Since  $\|\mathbf{k}_i\| = \|\mathbf{q}\| = 1$ , we have  $\frac{1}{2}\|\mathbf{k}_i - \mathbf{q}\|^2 = 1 - \mathbf{k}_i^\top \mathbf{q}$ . The  $r$ -weight polynomial kernel is defined as:

$$K_h(\mathbf{k}_i - \mathbf{q}) = \left[ 1 - \frac{\|\mathbf{k}_i - \mathbf{q}\|^2}{h^2} \right]_+^r \quad (23)$$

$$= \left[ 1 - \frac{2(1 - \mathbf{k}_i^\top \mathbf{q})}{h^2} \right]_+^r \quad (24)$$

$$= \left[ \frac{h^2 - 2 + 2\mathbf{k}_i^\top \mathbf{q}}{h^2} \right]_+^r. \quad (25)$$

That is, the induced kernel takes the form  $K_h(\mathbf{u}) \propto [1 - \|\mathbf{u}\|^2]_+^r$ , a rectified polynomial kernel of order  $r$ , encompassing classical kernels such as the biweight ( $r = 2$ ) and triweight ( $r = 3$ ). Now, introducing a temperature  $\gamma$ , the denominator in (17) can be expressed as

$$\sum_{i=1}^{n-1} \left[ 1 - \frac{\|\mathbf{k}_i - \mathbf{q}\|^2}{h^2} \right]_+^r = \left( \frac{2r\gamma}{h^2} \right)^r \sum_{i=1}^{n-1} \left[ \frac{h^2}{2r\gamma} - \frac{1}{r\gamma} + \frac{\mathbf{k}_i^\top \mathbf{q}}{r\gamma} \right]_+^r. \quad (26)$$

Choosing  $h$  such that

$$\sum_{i=1}^{n-1} \left[ \frac{\mathbf{k}_i^\top \mathbf{q}}{r\gamma} - \underbrace{\left( \frac{1}{r\gamma} - \frac{h^2}{2r\gamma} \right)}_{:=\tau} \right]_+^r = 1, \quad (27)$$

the normalizer  $\tau = \frac{1}{r\gamma} - \frac{h^2}{2r\gamma}$  coincides with the  $\alpha$ -entmax threshold (4), yielding

$$\hat{\mathbf{v}}_n(\mathbf{q}) = \sum_{i=1}^{n-1} \alpha\text{-entmax}_i \left( \frac{\mathbf{K}\mathbf{q}}{\gamma} \right) \mathbf{v}_i, \quad (28)$$

with an adaptive bandwidth  $h = \sqrt{2 - 2r\gamma\tau}$ . □

## B. Experimental Details

### B.1. Language Modeling

In this section, we provide additional details of our experimental setup, including model configurations and training hyperparameters for the language modeling task (Table 3). We also show the full training and validation curves for the BabiStories dataset (see statistics in Table 4) (Zhang et al., 2025), complementing the results in the main text (Figure 3). All models use the GPT-2 tokenizer (Radford et al., 2019) and share a sequence length of 512 tokens. Experiments cover different numbers of parallel layers of persistent and contextual memories. For single-layer models, we vary  $k \in 16, 32, 64$  and report results for the best-performing value ( $k = 32$ ), which is then used for all multi-layer configurations. Each contextual memory unit computes leaky-average keys and one-step-ahead values, with retrieval performed via kernel-weighted interpolation over past embeddings. All models are trained for 80k iterations with a global batch size of 512, optimized with Adam, and using learning rate schedules consistent with GPT-2 Small (Radford et al., 2019). For 12-layer models, the learning rate is reduced to  $10^{-3}$ . Sparse attention patterns for the rectified polynomial kernels are learned efficiently using AdaSplash (Gonçalves et al., 2025). While in practice the normalized ReLU is not often met, we use uniform weighting for those cases.

### B.2. In-Context Learning

For evaluation, we use RegBench (Akyürek et al., 2024). RegBench constructs random artificial languages defined by a PFA. Each input sequence consists of 10–20 strings sampled from the same PFA, separated by special delimiter tokens.

Table 3. Main training and model hyperparameters across model depths. Unless otherwise specified, hyperparameters are shared across all experiments.

Hyperparameter	1 layer	8 layers	12 layers
<i>Optimization</i>			
Batch size (total)	512	512	512
Learning rate	$5 \times 10^{-3}$	$5 \times 10^{-3}$	$1 \times 10^{-3}$
Min learning rate	$1 \times 10^{-4}$	$1 \times 10^{-4}$	$5 \times 10^{-5}$
Max iterations	80k	80k	80k
Weight decay	0.1	0.1	0.1
Adam $\beta_1 / \beta_2$	0.9 / 0.95	0.9 / 0.95	0.9 / 0.95
Gradient clipping	1.0	1.0	1.0
<i>Learning rate schedule</i>			
Scheduler	Cosine decay		
Warmup iterations	2k		
LR decay iterations	80k		
<i>Model architecture</i>			
Context length ( $n$ )	512		
Embedding dimension ( $d$ )	768		
Attention heads	12		
<i>Persistent memory</i>			
Memory size	2688		

Table 4. BabiStories dataset statistics (Zhang et al., 2025).

Dataset partition	# Stories	# Tokens (GPT-2 tokenizer)	Avg. # Characters per story
Train	2.2M	474,704,907	888
Valid	2.2k	4,749,107	889

Models are evaluated on their ability to predict the last token of testing sequences generated from held-out PFAs, effectively measuring their capacity to generalize the underlying generative rules.

For Memory Mosaics, we perform a grid search over the Gaussian kernel hyperparameters, select the best configuration based on validation loss, and apply those hyperparameters to the remaining kernels. During the hyperparameter search for the Gaussian kernel variant, various configurations were tested, including different number of blocks and weight decay. Particular attention was given to the hyperparameters of the Memory Mosaics, such as the number of heads and embedding size. For kNN-based approaches, we tune  $k \in \{16, 32, 64\}$  on 1k training examples and use that value ( $k = 16$ ) for the remaining training datasets and for uniform kNN. All hyperparameters tested are shown in Table 5.

### B.3. Length Generalization

For biological agents, episodic memory scales with the length of life rather than a fixed context window, placing memory retrieval inherently in the long-context regime and requiring continual length generalization. In such settings, dense aggregation over all stored memories would lead to severe interference, motivating the use of sparse retrieval mechanisms that selectively engage only a small subset of relevant memories. This perspective aligns with hippocampal indexing theory, where retrieval operates over sparse indices rather than dense memory traces (Teyler & DiScenna, 1986; Goode et al., 2020). Inspired by this neurobiological constraint, we evaluate sparse attention mechanisms in a set of controlled synthetic tasks designed to isolate core sequence-modeling abilities. Specifically, we consider multi-query multi-token associative recall (MQMTAR), sequence reversal, and sequence sorting, which respectively probe long-range associative retrieval, sequential manipulation, and global reordering. To ensure comparability across tasks and focus on the effects of the attention mechanism itself, we fix all model hyperparameters to modest values rather than performing extensive task-specific tuning; the shared hyperparameters are summarized in Table 6. We show in Table 7 additional results for different  $k$  for the kNN

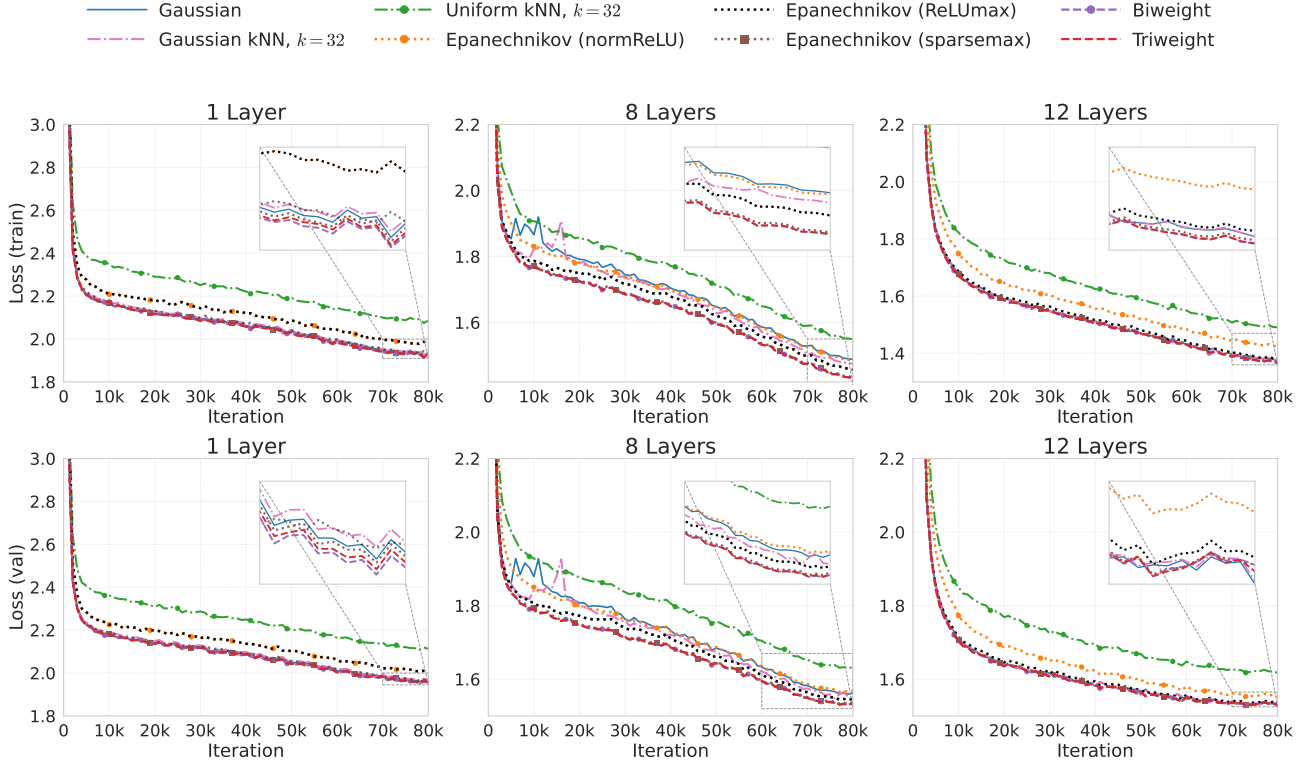


Figure 3. Training and validation loss of Memory Mosaic models with different kernels. Comparison on the BabiStories dataset for varying model depths. The horizontal axis shows the number of training iterations.

variants.

**Multi-query Multi-token Associative Recall (MQMTAR).** The Multi-query Multi-token Associative Recall task evaluates a model’s ability to store and retrieve multiple key–value associations within a single sequence and to answer several queries in parallel. The vocabulary consists of 256 integers, augmented with utility tokens  $\{0, 1, 2\}$  and additional special tokens used for structural delimitation. Each key  $k_i$ , value  $v_i$ , and query  $q_j$  is represented by a fixed-length sequence of two discrete tokens, corresponding to two numbers drawn from the base vocabulary. During input construction, multiple key–value pairs  $(k_i, v_i)$  are presented sequentially, followed by a set of four query keys  $\{q_1, q_2, q_3, q_4\}$ , all sharing the same two-token structure as the keys seen during the context. The model’s objective is to retrieve, for each query  $q_j$ , the value  $v_i$  associated with the matching key  $k_i$  encountered earlier in the sequence. The target output is formed by concatenating the two-token representations of the four retrieved values in query order. This task jointly probes multi-token associative binding, robustness to interference across multiple stored associations, and the ability to perform accurate multi-query recall within a single forward pass.

**Reverse.** The reverse task evaluates a model’s ability to store and reproduce the elements of a discrete sequence in reverse order. The vocabulary consists of integers from 0 to 31, and additional special tokens used for structural delimitation.

During input construction, a sequence of integers  $(x_1, x_2, \dots, x_n)$  is presented to the model. The model’s objective is to output the sequence in reverse order  $(x_n, x_{n-1}, \dots, x_1)$ . This task probes the model’s ability to memorize and manipulate sequential information over short-to-moderate context lengths.

**Sort.** The sort task evaluates a model’s ability to correctly reorder a sequence of discrete tokens in ascending order. The vocabulary consists of integers from 0 to 31, including repetitions.

During input construction, a sequence of integers  $(x_1, x_2, \dots, x_n)$  is presented to the model. The model’s objective is to output the sequence sorted in non-decreasing order  $(y_1 \leq y_2 \leq \dots \leq y_n)$ . This task probes the model’s ability to maintain and manipulate sequential information over short-to-moderate context lengths.

Table 5. Hyperparameter space for the in-context learning experiment. Depth denotes the number of stacked blocks comprising persistent and contextual memories. Embedding size corresponds to the head dimension in transformers. We report results from the epoch achieving the lowest validation loss.

Parameter	Range
weight decay	$\{10^{-1}, 10^{-2}\}$
depth	$\{2, 4, 8\}$
embedding size	$\{32, 128, 256\}$
number of heads	$\{1, 2, 4, 8\}$
learning rate	$\{5 \times 10^{-4}\}$
maximum number of epochs	$\{200\}$
batch size	$\{32\}$

### Multi Query Multi Token Associative Recall (MQMTAR)

	$k_1$	$v_1$		$k_2$	$v_2$	$k_3$	$v_3$	$k_4$	$v_4$	$q_3$	$q_1$	$q_2$	$q_4$
Inputs: 0	73 58 1 106 177	0 209 116 1 131 31 0 195 61 1 248 216 0 256 174 1 60 14 0	$v_3$	216 104 1 147 101 260 2 256 174 2 73 58 2 195 61 2 216 104	$v_1$	$v_2$	$v_4$	$v_3$	$v_4$	$q_3$	$q_1$	$q_2$	$q_4$
Targets: 2 60 14 2 106 177 2 248 216 2 147 101													

### Reverse

Inputs: 22 16 12 2 5 26 31 6 20 3 9 14 24 4 8 1 28 0 17 4 7 28 2 20 24 24 11 16 24 14 26 2 3 31 20 22 4 16 10 20 4 8  
Targets: 8 4 20 10 16 4 22 20 31 3 2 26 14 24 16 11 24 24 20 2 28 7 4 17 0 28 1 8 4 24 14 9 3 20 6 31 26 5 2 12 16 22

### Sort

Inputs: 30 5 12 29 7 0 19 12 8 5 21 3 14 7 0 19 8 2 12 5 21 14 3 8 0 7 19 2 12 30  
Targets: 0 0 0 2 2 3 3 5 5 7 7 7 8 8 12 12 12 12 14 14 19 19 21 21 29 30 30

Figure 4. Illustration of the MQMTAR, reverse, and sort tasks. In the MQMTAR task, Soft colors indicate different keys, values, and queries for visual clarity. In the reverse task, the model receives a sequence of integers and must output them in reverse order. In the sort task, the model receives a sequence of integers and must output the sequence in ascending order.

## C. Additional Experiments

### C.1. Out-Of-Distribution

**Out-of-distribution generalization on Simple English Wikipedia.** Figure 5 compares the prediction performance of Memory Mosaics models trained on the BabiStories corpus and evaluated out-of-distribution on Simple English Wikipedia<sup>3</sup>. The reported curves correspond to an exponential moving average (EMA) of the token-wise cross-entropy loss, computed over previously observed tokens, which provides a smoothed estimate of predictive confidence as the sequence unfolds.

At the beginning of each sequence, the model has limited contextual information and operates in a high-uncertainty regime. In this early phase, all attention variants exhibit similar behavior, with rapidly decreasing loss as additional context is incorporated, although higher-order compact kernels such as biweight and triweight typically start from slightly lower loss values. This reflects the fact that, under uncertainty, strongly localized kernels may initially overperform dense Gaussian attention, which aggregates information more broadly.

As the sequence progresses and the model becomes more confident, clear differences emerge. Attention mechanisms based on compactly supported kernels—Epanechnikov, biweight, and triweight—consistently achieve comparable loss with Gaussian attention, indicating that localized, sparse aggregation promotes selective and context-relevant memory retrieval in out-of-distribution settings. Among these, ReLUMax performs best overall: by combining sparse support with max anchoring, it avoids empty-support degeneracies while retaining locality, yielding stable and robust generalization as contextual evidence accumulates.

<sup>3</sup><https://huggingface.co/datasets/rahular/simple-wikipedia>

Table 6. Hyperparameters used for MQMTAR recall, reverse, and sorting tasks. Hyperparameters were fixed to keep models simple and comparable.

Parameter	MQMTAR	Reverse	Sorting
Training examples	$50 \times 10^6$	$30 \times 10^6$	$40 \times 10^6$
# epochs	1	1	1
Vocab size	263	36	36
Weight decay	$10^{-1}$	$10^{-1}$	$10^{-1}$
Depth	4	4	2
Embedding size	512	512	512
Number of heads	8	8	8
Learning rate	$10^{-3}$	$10^{-3}$	$10^{-3}$
Batch size	256	256	256
Training sequence length	up to 64	64	64

Table 7. Exact match accuracy on representative synthetic tasks. In-distribution results ( $n = 64$ ) and out-of-distribution performance at increasing sequence lengths are reported. Values show the mean across three seeds, with the maximum across seeds indicated in superscript. Best average performance is in **bold** and overall maximum performance is underlined.  $L$  represents the number of layers.

Kernel	MQMTAR ( $L = 4$ )							Reverse ( $L = 4$ )			Sort ( $L = 2$ )		
	1×	2×	4×	8×	16×	32×	64×	1×	1.5×	1×	2×	4×	
Gaussian kNN, $k = 16$	<b>0.99</b> <sup>(1.00)</sup>	<b>0.97</b> <sup>(1.00)</sup>	<b>0.93</b> <sup>(0.99)</sup>	<b>0.85</b> <sup>(0.96)</sup>	0.65 <sup>(0.78)</sup>	0.25 <sup>(0.36)</sup>	<b>0.05</b> <sup>(0.09)</sup>	0.86 <sup>(1.00)</sup>	<b>0.00</b> <sup>(0.00)</sup>	<b>1.00</b> <sup>(1.00)</sup>	0.74 <sup>(0.89)</sup>	0.00 <sup>(0.00)</sup>	
Gaussian kNN, $k = 32$	<b>0.99</b> <sup>(1.00)</sup>	<b>0.97</b> <sup>(1.00)</sup>	<b>0.93</b> <sup>(0.99)</sup>	0.84 <sup>(0.96)</sup>	<b>0.68</b> <sup>(0.85)</sup>	<b>0.27</b> <sup>(0.36)</sup>	<b>0.05</b> <sup>(0.05)</sup>	<b>0.99</b> <sup>(1.00)</sup>	<b>0.00</b> <sup>(0.00)</sup>	<b>1.00</b> <sup>(1.00)</sup>	<b>0.80</b> <sup>(0.91)</sup>	<b>0.01</b> <sup>(0.02)</sup>	
Uniform kNN, $k = 16$	<b>0.58</b> <sup>(0.71)</sup>	<b>0.01</b> <sup>(0.01)</sup>	<b>0.00</b> <sup>(0.00)</sup>	<b>1.00</b> <sup>(1.00)</sup>	<b>0.41</b> <sup>(0.63)</sup>	<b>0.00</b> <sup>(0.00)</sup>							
Uniform kNN, $k = 32$	0.04 <sup>(0.08)</sup>	<b>0.00</b> <sup>(0.00)</sup>	0.00 <sup>(0.00)</sup>	<b>0.00</b> <sup>(0.00)</sup>	<b>0.00</b> <sup>(0.00)</sup>	<b>0.00</b> <sup>(0.00)</sup>	<b>0.00</b> <sup>(0.00)</sup>	<b>0.42</b> <sup>(0.66)</sup>	<b>0.00</b> <sup>(0.00)</sup>	<b>1.00</b> <sup>(1.00)</sup>	0.00 <sup>(0.00)</sup>	<b>0.00</b> <sup>(0.00)</sup>	

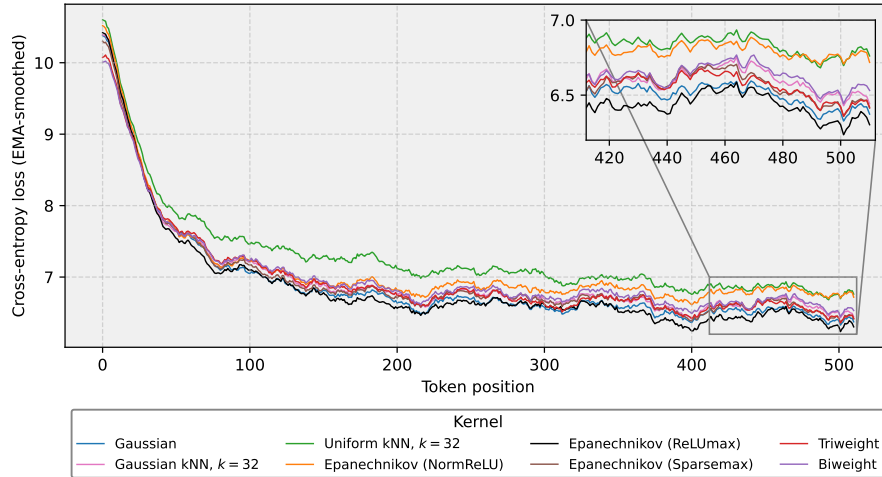


Figure 5. Prediction performance on the Simple English Wikipedia dataset using models trained on the BABISTORIES corpus. The plot reports the per-token average loss as a function of the token position within a 512-token input sequence.